This article was downloaded by:
On: *25 January 2011*
Access details: *Access Details: Free Access*
Publisher *Taylor & Francis*
Informa Ltd Registered in England and Wales Registered Number: 1072954 Registered office: Mortimer House, 37-41 Mortimer Street, London W1T 3JH, UK

Liquid Crystals
Publication details, including instructions for authors and subscription information:
http://www.informaworld.com/smpp/title~content=t713926090

Ferroelectric and antiferroelectric liquid crystals of chiral swallow-tailed materials with an ester group linked to achiral alkyl chains

S. -L. Wu[a]; T. -C. Lin[a]
[a] Department of Chemical Engineering Tatung University 40 Chungshan N. Rd., 3rd Sec. Taipei 104, Taiwan, ROC,

Online publication date: 11 November 2010

To cite this Article Wu, S. -L. and Lin, T. -C.(2004) 'Ferroelectric and antiferroelectric liquid crystals of chiral swallow-tailed materials with an ester group linked to achiral alkyl chains', Liquid Crystals, 31: 11, 1469 — 1477
To link to this Article: DOI: 10.1080/02678290412331298058
URL: http://dx.doi.org/10.1080/02678290412331298058

PLEASE SCROLL DOWN FOR ARTICLE

Full terms and conditions of use: http://www.informaworld.com/terms-and-conditions-of-access.pdf

This article may be used for research, teaching and private study purposes. Any substantial or systematic reproduction, re-distribution, re-selling, loan or sub-licensing, systematic supply or distribution in any form to anyone is expressly forbidden.

The publisher does not give any warranty express or implied or make any representation that the contents will be complete or accurate or up to date. The accuracy of any instructions, formulae and drug doses should be independently verified with primary sources. The publisher shall not be liable for any loss, actions, claims, proceedings, demand or costs or damages whatsoever or howsoever caused arising directly or indirectly in connection with or arising out of the use of this material.

LIQUID CRYSTALS, VOL. 31, NO. 11, NOVEMBER 2004, 1469–1477

Taylor & Francis
Taylor & Francis Group

Ferroelectric and antiferroelectric liquid crystals of chiral swallow-tailed materials with an ester group linked to achiral alkyl chains

S.-L. WU* and T.-C. LIN

Department of Chemical Engineering, Tatung University, 40 Chungshan N. Rd., 3rd Sec., Taipei 104, Taiwan, ROC

(*Received 31 March 2004; accepted 20 June 2004*)

Two homologous series of chiral materials, 3-pentyl (*S*)-2-{6-[4-(4′-alkanoyloxyphenyl)benzoyloxy]-2-napthyl}propionate, P*m*PBNP(*m* = 7–11), and 2-ethyl-1-butyl (*S*)-2-{6-[4-(4′-alkanoyloxyphenyl)benzoyloxy]2-napthyl}propionate, EB*m*PBNP(*m* = 7–11), derived from a chiral moiety, (*S*)-2-(6-methoxynaphthyl-2)propionic acid, in conjugation with swallow-tailed groups attached to the external side of the chiral centre, have been synthesized and their mesomorphic phases studied. Members of the P*m*PBNP series, with the exception of P7PBNP and P8PBNP, showed an enantiotropic antiferroelectric SmC^*_A phase; whereas, members of the EB*m*PBNP series, with the exception of EB7PBNP, showed an enantiotropic ferroelectric SmC* phase. The maximum spontaneous polarization for these materials was in the range 20–60 nC cm^{-2}. The electro-optic responses measured for both series of materials in ferroelectric and antiferroelectric phases displayed thresholdless V-shaped switching.

Downloaded At: 16:42 25 January 2011

1. Introduction

The first report of thresholdless, hysteresis-free, V-shaped switching in an antiferroelectric mixture was made by Inui *et al.* [1]. This switching mode provides attractive displays characterized by a wide viewing angle, a large contrast ratio, high speed response and an ideal analogue grey scale with no hysteresis [2]. Subsequently, thresholdless, V-shaped switching in chiral smectic liquid crystals have became an active subject for research. Extended studies on the Inui mixture showed that the V-shaped switching behaviour strongly depends on the alignment layer thickness and type of polyimide, cell gap, and applied frequency [1, 3–6]. Only a few studies, however, have reported on the effect of liquid crystals molecular structure on this switching behavior [7–9].

Our previous studies showed that chiral swallow-tailed materials (*S*)-EP*m*PBNP possess antiferroelectricity with thresholdless, V-shaped switching [7, 10]. This finding provided a means of investigating the influence on switching mode of variation in molecular structure. It is worthy of note that achiral materials with swallow-tailed terminal moieties have been demonstrated to possess the SmC_{alt} phase with antiferroelectric-like structure [11]. Thus, in order to understand further the effect of molecular structure on mesomorphic and electro-optical properties, we have designed and synthesized two new series of chiral materials that have structures similar to (*S*)-EP*m*PBNP, by the replacement of an ether linkage with an ester linkage to the achiral peripheral alky chain. The general structural formulae of the two new chiral swallow-tailed materials, P*m*PBNP and EB*m*PBNP, are depicted below.

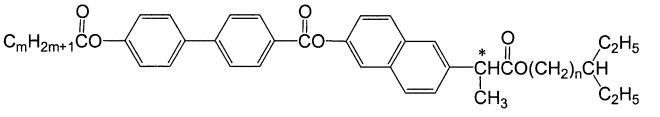

P*m*PBNP: (*m*=7~11, n=0)

EB*m*PBNP: (*m*=7~11, n=1)

2. Experimental

2.1. *Characterization of materials*

The structures of the intermediates and final products were checked by thin layer chromatography and further identified by nuclear magnetic resonance spectroscopy using a Bruker AVANCE 500 NMR (^{1}H NMR, 500 MHz) spectrometer. The purity of the final products was confirmed by elemental analysis using a Perkin-Elmer 2400 instrument. Percentage errors in the carbon and hydrogen results for the target compounds were less than 1% as compared with calculated figures. The phase transition temperatures and associated

*Author for correspondence; e-mail: slwu@ttu.edu.tw

Liquid Crystals ISSN 0267-8292 print/ISSN 1366-5855 online © 2004 Taylor & Francis Ltd
http://www.tandf.co.uk/journals
DOI: 10.1080/02678290412331298058

transition enthalpies of the compounds were determined by differential scanning calorimetry (DSC) using a Perkin-Elmer DSC 7 at a running rate of 5°C min^{-1}. Mesophases were identified using a Nikon Microphot-FXA optical microscope in conjunction with a Mettler FP82-HT hot stage controlled by Mettler FP90 control processor. Commercial homogenous cells coated with polyimide as alignment film were purchased from E. H. C. Co. Ltd, Japan and Linkam Scientific Instruments Ltd, UK. The sample was filled into the cell by capillary action in the isotropic state. Conducting wires were fixed separately to the ITO-coated glass plates of the sample cell by silver paint.

Spontaneous polarization ($\mathbf{P}_s$) was measured by the triangular wave method [12], using a Yogawa AG1200 arbitrary waveform generator with amplification by an NF Electronics Instrument 4005 power amplifier. Currents were measured by detecting the voltage change across a resistor of 50 kΩ, using a HP 54502A digital oscilloscope to monitor the signals. The dispersion curves were measured with a HP 4284A precision LCR meter.

The measurement of optical transmittance versus applied electric field was conducted by using a He-Ne laser (5 mW, 632.8 nm) as a probe beam [13, 14]. The optical transmittance of the probe beam passing through the cell between crossed polarizers, whose axes were parallel and perpendicular to the smectic layer normal, was detected by a photodiode.

Downloaded At: 16:42 25 January 2011

2.2. *Preparation of materials*

The starting chiral compound for the synthesis of compounds P*m*PBNP and EB*m*PBNP was (*S*)-2-(6-methoxynaphthyl-2)propionic acid, purchased from Tokyo Chemical Industry Co. Ltd, Japan, with optical purity greater than 99% enantiomeric excess. The synthetic procedures for P*m*PBNP and EB*m*PBNP compounds were carried out in the same manner as described in a previous paper and are shown in the scheme [15]. Typical examples of synthetic details are given below.

2.2.1. *4-(4′-Alkanoyloxyphenyl)benzoic acids, mPBA(m = 7–11)*

Alkanoyl chloride (14 mmol) was slowly added to a solution of 4′-hydroxybiphenyl-4-carboxylic acid (17 mmol) in dried pyridine/dichloromethane (1/6). The reaction mixture was stirred under reflux for 5 h, then added to a solution of hydrochloric acid in water under cooled in an ice-water bath. The precipitate was filtered off and recrystallized from ethanol; yields 60–70%. A typical ^{1}H NMR ($CDCl_3$) analytics for *m*PBA(*m* = 11) spectrum is given as follow: δ (ppm) 0.87–0.90 (t, 3H, $(CH_2)_8C\mathbf{H}_3$), 1.28–1.43 (m, 16H , $(C\mathbf{H}_2)_8CH_3$), 1.76–1.79 (m, 2H, $C\mathbf{H}_2CH_2COO$), 2.58–2.61 (t, 2H, $CH_2C\mathbf{H}_2COO$), 7.19–7.20 (d, 2H, Ar**H**), 7.63–7.68 (dd, 4H, Ar**H**), 8.16–8.18 (d, 2H, Ar**H**).

2.2.2. *3-Pentyl (S)-2-(6-methoxy-2-naphthyl)propionate, PMNP*

(*S*)-2-(6-methoxy-2-naphthyl)propionic acid (25 mmol) and 3-pentanol (22 mmol) were dissolved in dry dichloromethane (100 ml). After the addition of dicyclohexylcarbaimide (DCC, 25 mmol) and dimethylaminopyridine (DMAP, 2.2 mmol) the solution was stirred at room temperature for 5 days. The precipitates were filtered off and washed with dichloromethane. The filtrate was successively washed with 5% acetic acid, 5% aqueous sodium hydroxide and water, and then dried over anhydrous magnesium sulphate and concentrated under vacuum. The residue was purified by column chromatography on silica gel (70–230 mesh) using dichloromethane as eluant. The isolated ester was an oily liquid; yield 85%. ^{1}H NMR ($CDCl_3$): δ (ppm) 0.65–0.68 (t, 3H, $CH_2C\mathbf{H_3}$), 0.83–0.86 (t, 3H, $CH_2C\mathbf{H}_3$), 1.42–1.48 (m, 4H, $CH(C\mathbf{H}_2CH_3)_2$), 1.53–1.59 (d, 3H, $ArCH(C\mathbf{H}_3)COO$), 3.83–3.87 (q, 1H, $ArC\mathbf{H}(CH_3)COO$), 3.92 (s, 3H, $C\mathbf{H}_3O$), 4.73–4.78 (m, 1H, $COOC\mathbf{H}$), 7.11–7.14 (m, 2H, Ar**H**), 7.41–7.43 (dd, 1H, Ar**H**), 7.68–7.71 (m, 3H, Ar**H**).

2.2.3. *2-Ethyl-1-butyl (S)-2-(6-methoxy-2-naphthyl)propionate, EBMNP*

The synthetic procedures were the same as described for PMNP; yield 85%. ^{1}H NMR ($CDCl_3$): δ (ppm) 0.78–0.83 (q, 6H, $CH(CH_2C\mathbf{H}_3)_2$), 1.22–1.28 (m, 4H, $CH_2CH(C\mathbf{H}_2CH_3)_2$), 1.43–1.48 (m, 1H, $CH_2C\mathbf{H}$-$(CH_2CH_3)_2$), 1.57–1.59 (d, 3H, $ArCH(C\mathbf{H}_3)COO$), 3.85–3.86 (q, 1H, $ArC\mathbf{H}(CH_3)COO$), 3.92 (s, 3H, $C\mathbf{H}_3O$), 3.99–4.00 (d, 2H, $COOC\mathbf{H}_2CH$), 7.11–7.14 (m, 2H, Ar**H**), 7.39–7.41 (dd, 1H, Ar**H**), 7.66–7.70 (t, 3H, Ar**H**).

2.2.4. *3-Pentyl (S)-2-(6-hydroxy-2-naphthyl)propionate, PHNP*

The ester PMNP (17 mmol) dissolved in dry dichloromethane (62 ml) was mixed with BBr_3 (32 mmol) at −20°C for 5 min, and at 0°C for 1 h. After diluting with dichloromethane (124 ml), the solution was poured into a mixture of saturated aqueous ammonium chloride (62 ml) and ice chips (62 g). The organic layer was separated and washed with brine ice, dried over anhydrous sodium sulphate, and concentrated under vacuum. The residue was purified by silica gel (70–230 mesh) column chromatography using dichloromethane as

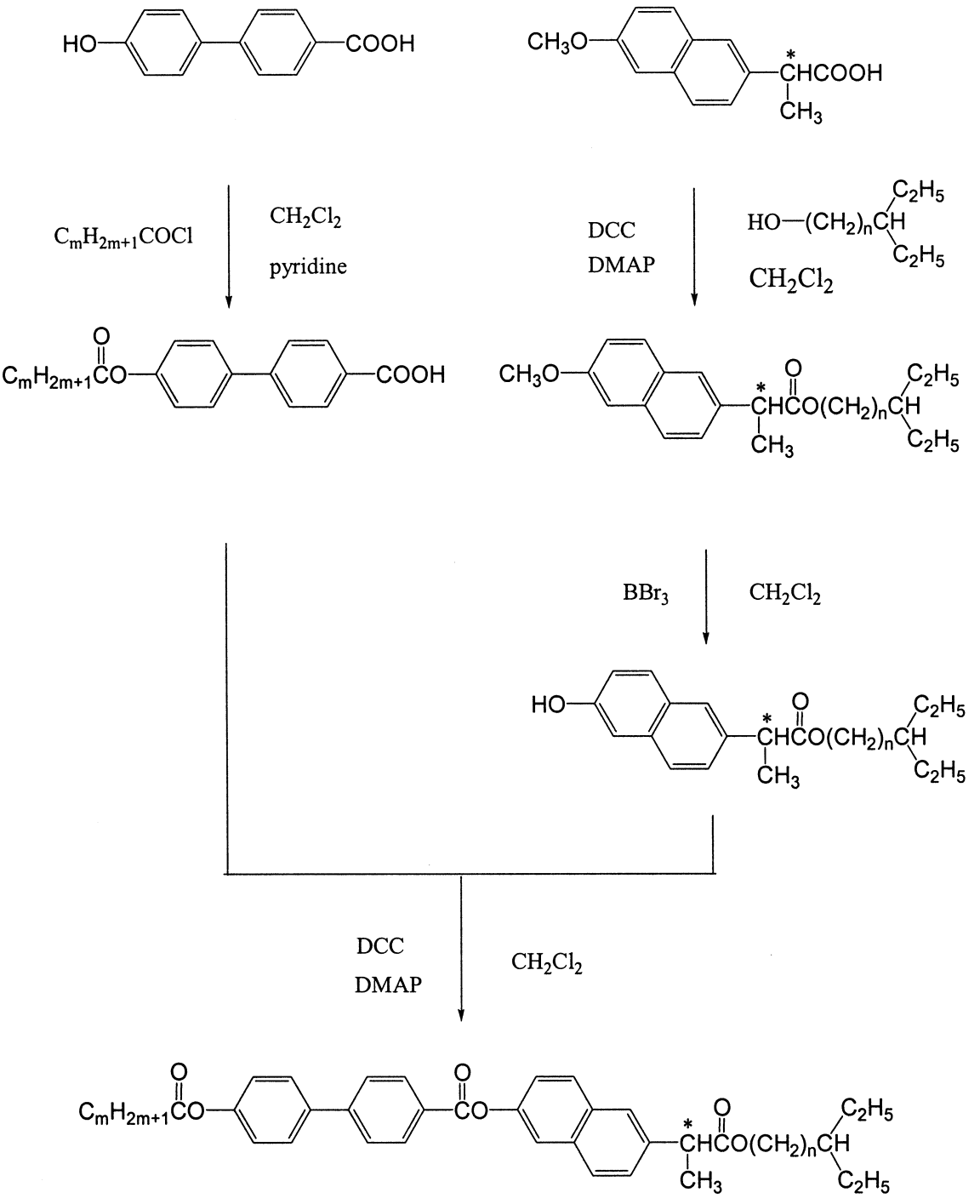

P*m*PBNP: (*m*=7~11, n=0)
EB*m*PBNP: (*m*=7~11, n=1)

Scheme. Synthetic procedures for the target materials P*m*PBNP and EB*m*PBNP.

Downloaded At: 16:42 25 January 2011

eluant. The alcohol PHNP was collected after recrystallization from hexane; yield 40%. ^{1}H NMR ($CDCl_3$): δ (ppm) 0.66–0.69 (t, 3H, CH_2CH_3), 0.83–0.86 (t, 3H, CH_2CH_3), 1.42–1.48 (m, 4H, $CH(CH_2CH_3)_2$), 1.54–1.58 (d, 3H, $ArCH(CH_3)COO$), 3.82–3.86 (q, 1H, $ArCH(CH_3)COO$), 4.74–4.77 (m, 1H, COOCH), 5.06 (s, 1H, OH), 7.07–7.09 (dd, 1H, ArH), 7.11, (d, 1H, ArH), 7.40–7.41, (dd, 1H, ArH), 7.61–7.63 (d, 1H, ArH), 7.67–7.71 (t, 2H, ArH).

2.2.5. *2-Ethyl-1-butyl (S)-2-(6-methoxy-2-naphthyl)propionate, EBHN*

The synthetic procedures for EBHN were the same as described for PHNP; yield 60–70%. ^{1}H NMR ($CDCl_3$): δ (ppm) 0.79–0.83 (t, 6H, $CH(CH_2CH_3)_2$), 1.24–1.29 (m, 4H, $CH(CH_2CH_3)_2$), 1.44–1.49 (m, 1H, $COOCH_2CH(CH_2)_2$), 1.57–1.60 (m, 3H, $ArCH(CH_3)COO$), 3.85–3.86 (q, 1H, $ArCH(CH_3)COO$), 4.00–4.01 (d, 2H, $COOCH_2CH$), 5.06 (s, 1H, OH), 7.08–7.10 (dd, 1H, ArH), 7.12 (d, 1H, ArH), 7.39–7.41 (dd, 1H, ArH), 7.63–7.64 (d, 1H, ArH), 7.67 (s, 1H, ArH), 7.70–7.72 (d, 1H, ArH).

2.2.6. *3-Pentyl (S)-2-{6-[4-(4′-alkanoyloxyphenyl)benzoyloxy]-2-napthyl}propionates, PmPBNP*

The esters P*m*PBNP ($m=7$–11) were synthesized in the same manner as described for esters PMNP. A mixture of *m*PBA (1.9 mmol), alcohol PHNP (1.7 mmol), DCC (1.9 mmol), DMAP (1.7 mmol) and dry dichloromethane (10 ml) was stirred at room temperature for 5 days. After purification, 40–50% yields of products were obtained. All materials were analysed and identified satisfactorily. A typical example of analytical data for P11BNP is as follows. Elemental analysis: calculated, C 77.68, H 7.88; found, C 77.39, H 0.37. ^{1}H NMR ($CDCl_3$): δ (ppm) 0.66–0.69 (t, 3H, RCH_3), 0.84–0.90 (m, 6H, $CH(CH_2CH_3)_2$), 1.28–1.62 (m, 23H, $(CH_2)_{m-3}$, $CH(CH_3)$), 1.77–1.80 (m, 2H, CH_2CH_2COO), 2.58–2.61 (t, 2H, CH_2CH_2COO), 3.89–3.91 (q, H, $ArCH(CH_3)COO$), 4.76–4.77 (m, H, COOCH), 7.21–8.32 (m, 14H, ArH).

2.2.7. *2-Ethyl-1-butyl (S)-2-{6-[4-(4′-alkanoyloxyphenyl)benzoyloxy]-2-napthyl}propionates, EBmPBNP*

The synthetic procedures for EB*m*PBNP were the same as described for P*m*PBNP; yields were 40–50%. All materials were analysed and identified satisfactorily. A typical example of analytical data for EB11PBNP is as follows. Elemental analysis: calculated, C 77.84, H 8.02; found, C 77.70, H 8.03. ^{1}H NMR ($CDCl_3$): δ (ppm) 0.79–0.84 (m, 6H, $CH(CH_2CH_3)_2$), 0.87–0.90 (t, 3H, RCH_3), 1.23–1.79 (m, 24H, $(CH_2)_{m-3}$, $CH(CH_3)$), 1.76–1.82 (m, 2H, CH_2CH_2COO), 2.17–2.61 (t, 2H, CH_2CH_2COO), 3.88–3.93 (q, 1H, $ArCH(CH_3)COO$), 4.01–4.02 (d, 2H, $COOCH_2$), 7.21–8.32 (m, 14H, ArH).

3. Results and discussion

Microscopic textures were primarily used for the identification of the mesophases. In the case of compounds P*m*PBNP, on cooling from the isotropic liquid, the N* phase was characterized by the formation of a scale-like or fan-like texture. On further cooling, a texture of spiral filaments appeared and was identified by the characteristics of the TGB_A^* phase [16–18]. The SmA* phase was characterized by the formation of a pseudo-homeotropic texture, and the SmC_A^* phase was characterized by the formation of a petal texture. In the case of compounds EB*m*PBNP, the N* phase was demonstrated by the formation of a scale-like or fan-like texture. The SmA* and SmC* phases were characterized by pseudo-homeotropic texture and four-brush defect in the schlieren texture, respectively.

The mesophase, transition temperatures, and enthalpies of transition for P*m*PBNP and EB*m*PBNP are listed in tables 1 and 2, respectively. Phase diagrams of the transition temperature plotted against the number of carbon atoms in the achiral chain are shown in figures 1 and 2 for each series of materials. Three P*m*PBNP compounds ($m=9$–11) exhibited an enantiotropic SmC_A^* phase, its thermal stability increasing as n increased. Four EB*m*PBNP compounds ($m=8$–11) exhibited an enantiotropic SmC* phase, its phase range increasing with increasing terminal achiral chain length. The unidentified CrX* crystalline phase in the P*m*PBNP series appears when the achiral chain length is below 9, whereas unidentified CrX* crystalline phase appears in all EB*m*PBNP compounds. The melting points of the two series of compounds are approximately the same, but the EB*m*PBNP clearing temperature is much lower than that of the P*m*PBNP, suggesting that an additional methylene group ($n=1$) could lower the clearing points. In addition, an additional methylene group suppresses the formation of the TGB_A* phase and alters the antiferroelectric SmC_A^* phase to a ferroelectric SmC* phase. EB*m*PBNP compounds show a narrower N* phase than the P*m*PBNP series, while they have a preference to form the CrX* phase, as compared with the P*m*PBNP compounds.

In order to confirm the existence of the SmC_A^* phase for P*m*PBN, a miscibility study was performed by choosing a structural similar chiral material, (*S*)-EP10PBNP, which was previously proven to exhibit the SmC_A^* phase [10], as a standard material for the

Downloaded At: 16:42 25 January 2011

Table 1. Transition temperature T (°C) and enthalpies ΔH (kJ mol^{-1}, in italics) of the transition for materials P*m*PBNP(*m* = 7–11) at 5°C min^{-1} scanning rate.

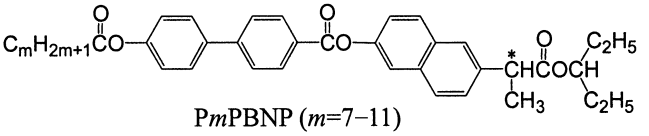

P*m*PBNP (*m*=7–11)

m	I		N*		TGB_A^*		SmA*		SmC_A^*		CrX		Cr	M.p.[c]
7	•	162.7	•	139.3	•	136.3	•	75.4	—		•	54.1	•	89.9
		1.03		*0.79*		[a]		*4.02*				*12.5*		*12.8*
8	•	156.4	•	138.1	•	135.2	•	55.1	—		•	45.9	•	81.9
		1.31		*0.54*		[a]		*1.37*				*19.8*		*27.9*
9	•	153.7	•	138.2	•	135.8	•	104.3	•	42.1	—		•	82.6
		0.32		*0.39*		[a]		[b]		*22.9*				*25.8*
10	•	149.0	•	134.8	•	132.7	•	111.6	•	39.2	—		•	82.4
		0.72		*0.29*		[a]		*0.07*		*3.77*				*25.4*
11	•	146.0	•	134.3	•	133.9	•	115.0	•	44.8	—		•	88.2
		1.06		*0.26*		[a]		*0.07*		*20.8*				*27.7*

[a]The enthalpy of the TGB_A^*–SmA* transition was added to that of the N*–TGB_A^* transition.
[b]The enthalpy was too small to be measured.
[c]M.p. refers to the melting point taken from DSC thermograms, recorded at heating rates of 5°C min^{-1}.

Downloaded At: 16:42 25 January 2011

Table 2. Transition temperature T (°C) and enthalpies ΔH (kJ mol^{-1}, in italics) of the transition for materials EB*m*PBNP(*m* = 7–11) at 5°C min^{-1} scanning rate.

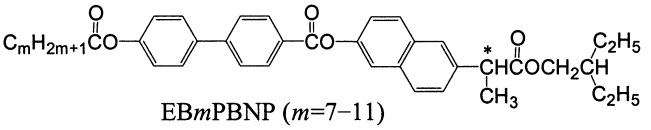

EB*m*PBNP (*m*=7–11)

EB*m*PBNP (*m* = 7–11)

m	I		N*		SmA*		SmC*		CrX		Cr	M.p.[b]
7	•	133.9	•	133.4	•	76.9	—		•	53.9	•	92.3
		2.1		[a]		*2.4*				*5.1*		*15.9*
8	•	129.8	•	128.2	•	110.0	•	66.6	•	42.3	•	91.9
		2.8		[a]		*0.08*		*3.1*		*9.2*		*25.2*
9	•	128.6	•	128.1	•	111.6	•	61.0	•	51.5	•	85.7
		2.9		[a]		*0.05*		*2.8*		*25.1*		*6.4*
10	•	127.6	•	125.7	•	115.3	•	53.0	•	24.6	•	87.9
		2.7		[a]		*0.53*		*4.6*		*8.4*		*29.0*
11	•	123.9	•	123.5	•	116.5	•	51.5	•	36.4	•	83.6
		1.83		[a]		*0.46*		*3.8*		*7.5*		*8.0*

[a]The enthalpies of I–N* and N*–SmA* transitions were added to that of the I–N* transition.
[b]M.p. refers to the melting point taken from DSC thermograms, recorded at heating rates of 5°C min^{-1}.

study. The mesophases and transition temperatures (°C) of (*S*)-EP10PBNP are as follow: I 143.1 BP_{II} 134.4 N* 129.0 TGB_A^* 128.2 SmA* 102.5 SmC_A^* 54.2 Cr. The testing sample, P9PBN, was mixed with the standard sample by varying weight percentage, and a phase diagram constructed of the binary mixtures as shown in figure 3. This phase diagram displays continuous miscibility of the SmC_A^* phase across the full composition range, supporting the assignment of existing SmC_A^* phase for P*m*PBN.

More detail studies of the SmC_A^* and SmC* phases for P*m*PBN and EB*m*PBNP compounds were conducted by investigation of the macro- and micro-molecular motions of the molecules. Thus, the

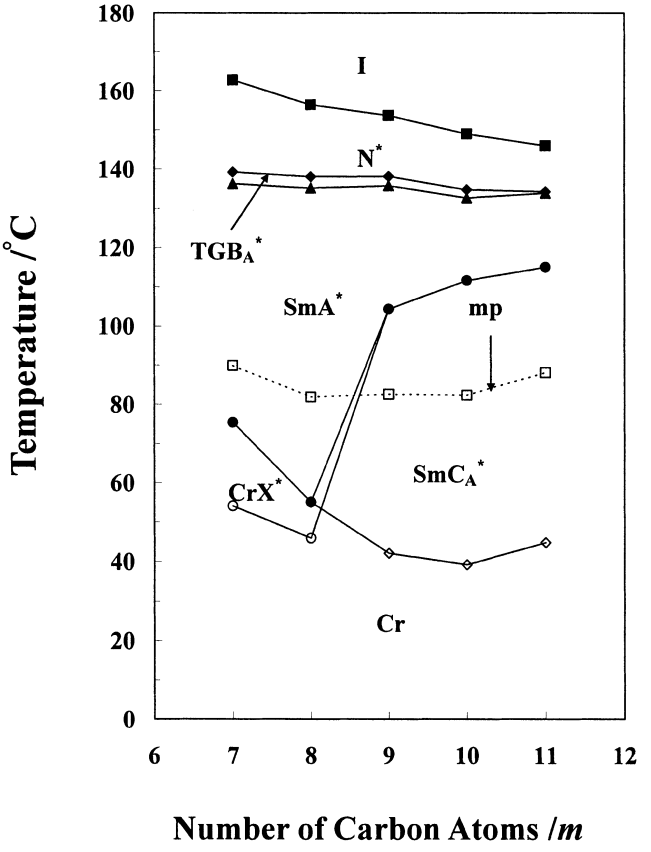

Figure 1. Phase diagram plotted by the number of carbon atoms in the achiral chain versus transition temperature of P*m*PBNP.

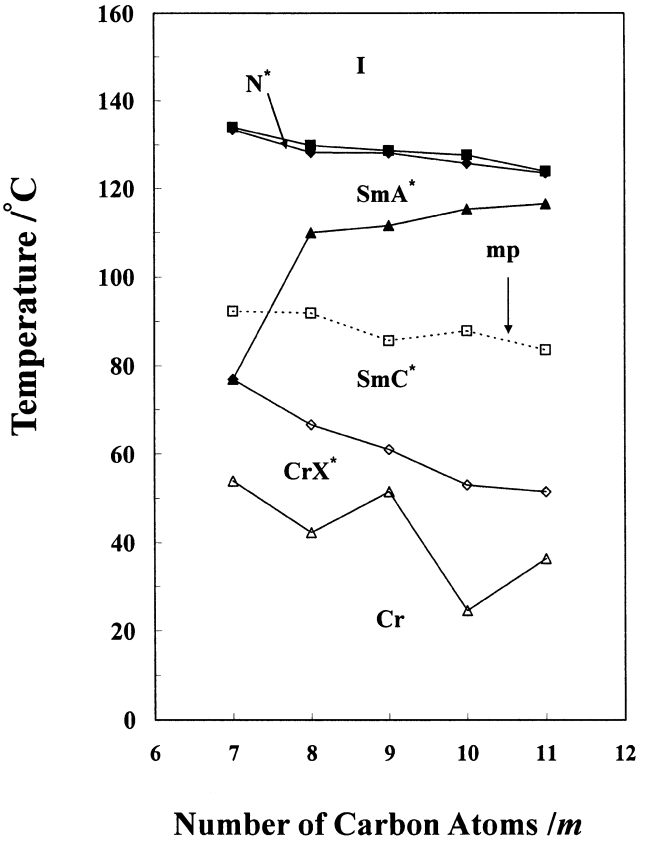

Figure 2. Phase diagram plotted by the number of carbon atoms in the achiral chain versus transition temperature of EB*m*PBNP.

Downloaded At: 16:42 25 January 2011

frequency dependence of dispersion and absorption curves was measured, with results for an example of P11PBN in the SmC_A^* phase as shown in figure 4. These results show that both the real and imaginary parts of the dielectric constants are quite unstable at a frequency < 1 kHz due to free charge contribution [19]. It can also be seen that the real part of the dielectric constant shows a tendency to diverge, accompanied with a consistent increase of the imaginary loss, at higher frequencies of 10^5–10^6 Hz. This feature is seen in the empty cell, and is presumably due to the effect of the polyimide and/or ITO films. Thus, there is no significant occurrence of a relaxation process in the SmC_A^* phase, as was detected in MHPOBC [20]. The frequency dependence of the dispersion and absorption curves was measured for EB11PBNP, with results shown in figure 5. One characteristic absorption peak of the SmC* phase is seen, due to the contribution of the Goldstone mode [21].

Spontaneous polarization ($\mathbf{P}_s$) for P*m*PBNP and EB*m*PBNP compounds was measured as a function of temperature on cooling in 5 μm homogenous cells, with results illustrated in figures 6 and 7, respectively. $\mathbf{P}_s$ of the SmC_A^* phase for compounds P*m*PBNP ($m = 9$–11), increases with decreasing temperature and reaches maximum values of 20–40 nC cm^{-2}, whereas compounds EB*m*PBNP ($m = 8$–11) possess maximum $\mathbf{P}_s$ values of 35–60 nC cm^{-2}. The results indicate that an additional methylene group between the chiral centre and swallow tail can increase the $\mathbf{P}_s$ value, as the conformation of the terminal chiral chain is more extended [22].

Optical transmittance versus electric field was measured for the P*m*PBNP and EB*m*PBNP series in 2 μm homogenous cells using an applied triangular waveform of varying frequency. The electro-optical response of P11PBNP at 1 Hz applied frequency shows hysteresis and W-shaped switching at the SmA* to SmC_A^* transition. On further lowering of the temperature, V-shaped switching occurs at 113°C, although a slight hysteresis was seen, as shown in figure 8. In the case of EB11PBNP, W-shaped switching behaviour also appears near SmA*–SmC* transition and then changes to V-shaped switching at 95°C, as shown in figure 9.

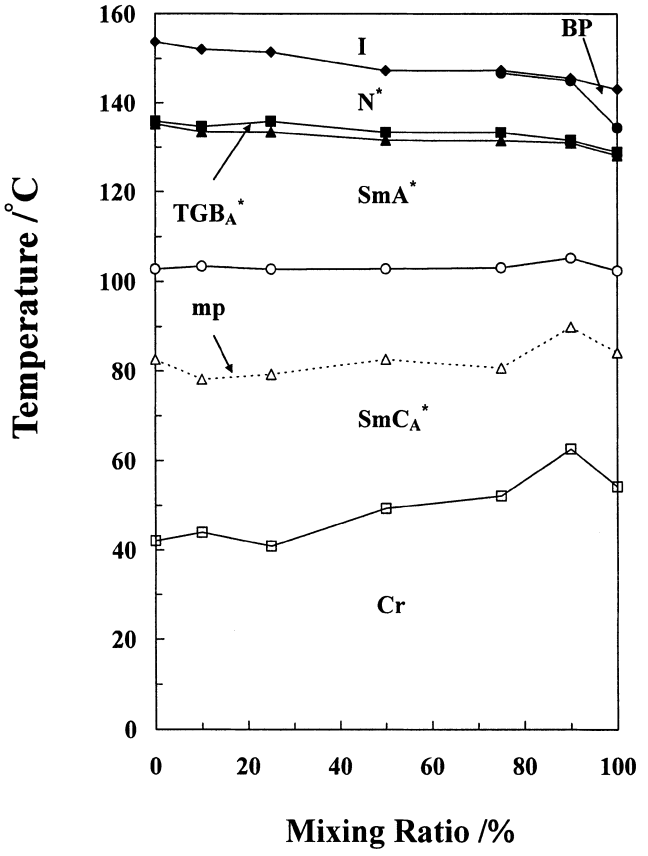

Figure 3. Miscibility phase diagram for mixtures (wt%) of standard sample (*S*)-EP10PBNP, and the testing sample P9PBNP.

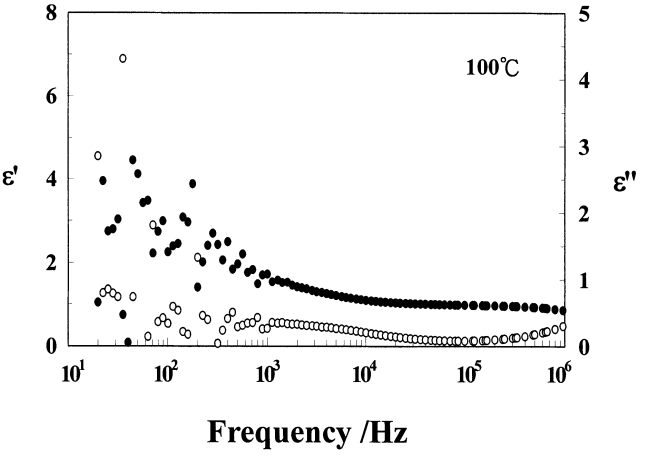

Figure 4. Frequency dependence curves for the dielectric dispersion (●) and absorption (○) measured in the SmC$_A^*$ phase of P11PBNP at 100°C.

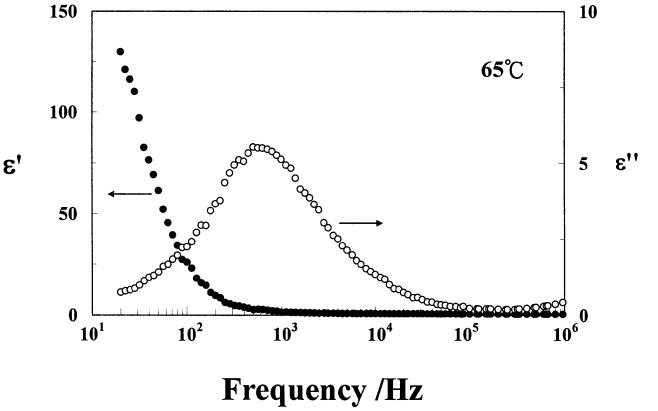

Figure 5. Frequency dependence curves for the dielectric dispersion (●) and absorption (○) measured in the SmC* phase of EB11PBNP at 65°C.

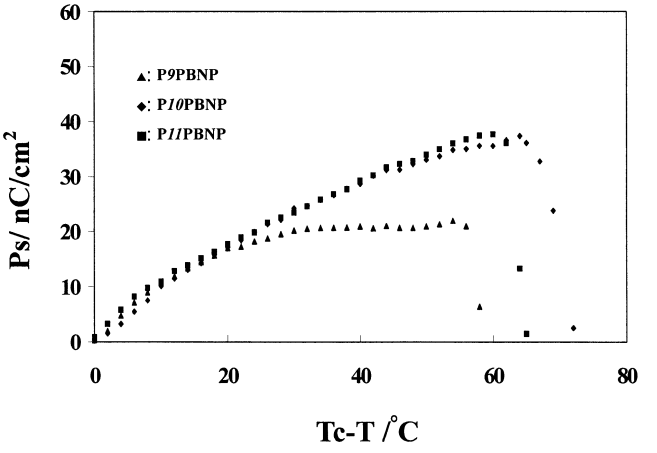

Figure 6. Spontaneous polarization plotted as a function of temperature for P*m*PBNP ($m=9$–11). T_c is the temperature of the SmA*–SmC$_A^*$ phase transition.

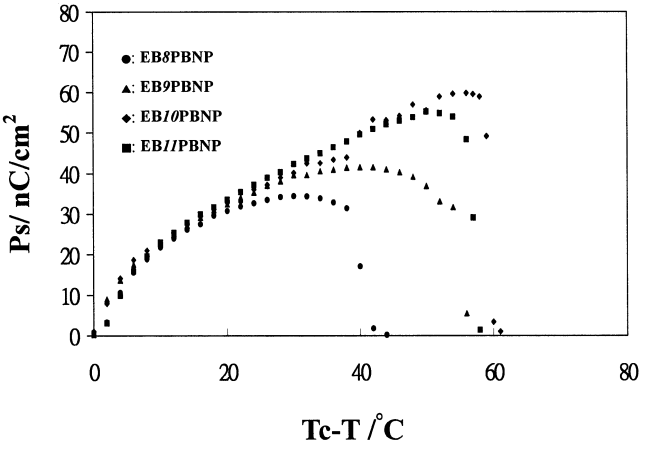

Figure 7. Spontaneous polarization plotted as a function of temperature for EB*m*PBNP ($m=8$–11). T_c is the temperature of the SmA*–SmC* phase transition.

Downloaded At: 16:42 25 January 2011

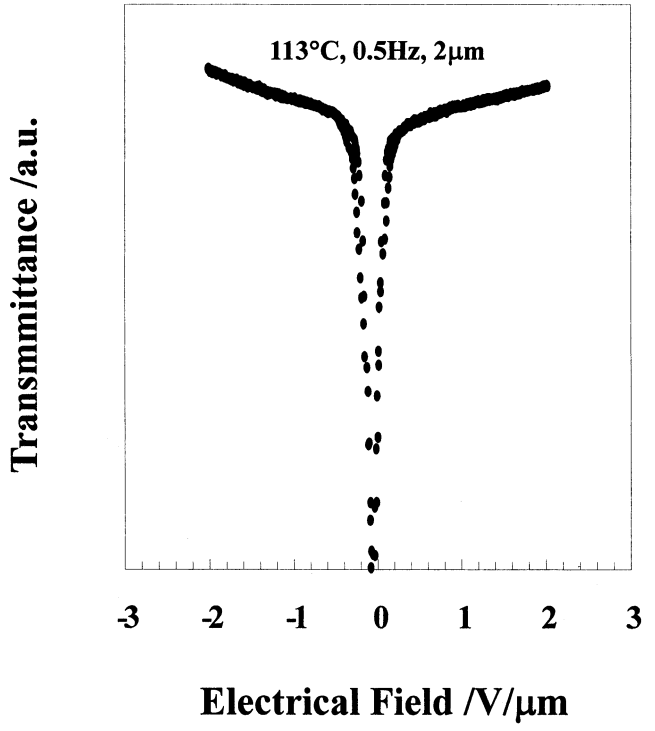

Figure 8. Optical transmittance as a function of applied electric field for P11PBNP, measured by applying a triangular waveform at 1 Hz frequency in 2 μm homogeneous cells at 111°C.

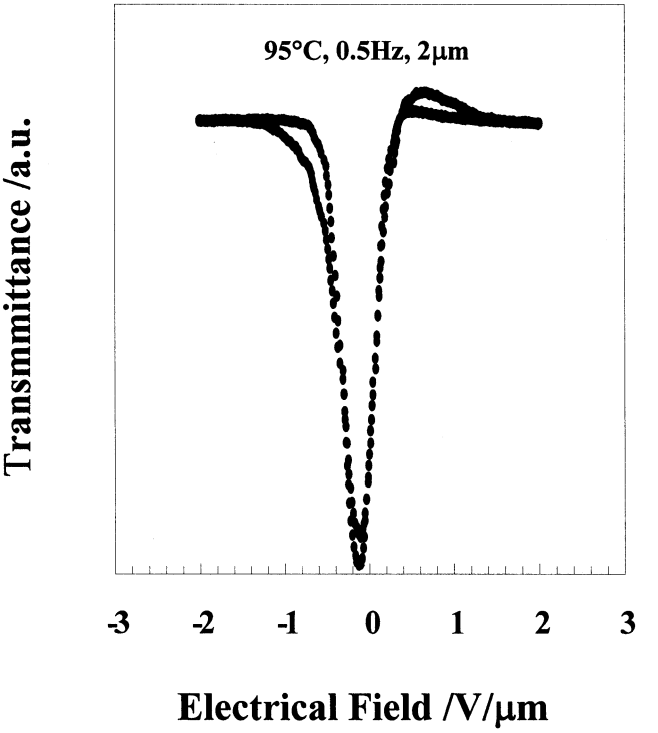

Figure 9. Optical transmittance as a function of applied electric field for EB11PBNP, measured by applying a triangular waveform at 0.5 Hz frequency in 2 μm homogeneous cells at 95°C.

Downloaded At: 16:42 25 January 2011

This clearly indicates that V-shaped switching behaviour critically depends on the phase temperature and the applied frequency. Moreover, V-shaped switching occurs in both the antiferroelectric and ferroelectric phases, with different magnitudes of spontaneous polarization, suggesting that this switching mode depends on the molecular structures themselves, but not the natures of the phases and the magnitudes of the molecular polarization.

4. Conclusion

Two structurally similar series of chiral materials, P*m*PBNP ($m=7$–11), and EB*m*PBNP ($m=7$–11), differ in the numbers of methylene groups (n = 0 or 1) between the swallow-tailed group and the chiral centre; experimental results indicated that P*m*PBNP ($m=9$–11) possesses an antiferroelectric SmC^*_A phase, while EB*m*PBNP ($m=8$–11) possesses a ferroelectric SmC* phase. It appeared that the formation of zigzag pairing in the smectic phase for the chiral liquid crystal has no relation to the swallow-tailed group of the molecules. The magnitudes of $\mathbf{P}_s$ values are different in these two series of materials; however, all materials displayed thresholdless, V-shaped switching properties, suggesting that this switching mode has no relation to the polarization of the molecules.

References

[1] Inui, S., Limura, N., Suruki, T., Iwane, H., Miyachi, F., Takanishi, Y., and Fukuda, A., 1996, *J. mater. Chem.*, **6,** 671.
[2] Saishu, T., Takatoh, K., Iida, R., Nagata, H., and Mori, Y., 1996, *SID'96 Dig.*, **28,** 4.
[3] Seomun, S. S., Takanishi, Y., Ishikawa, K., Takezoe, H., and Fukuda, A., 1997, *Jpn. J. appl. Phys.*, **36,** 3586.
[4] Seomun, S. S., Gouda, T., Takanishi, Y., Ishikawa, K., Takezoe, H., and Fukuda, A., 1999, *Liq. Cryst.*, **26,** 151.
[5] Chandani, A. D. L., Cui, Y., Seomun, S. S., Takanishi, Y., Ishikawa, K., and Takezoe, H., 1999, *Liq. Cryst.*, **26,** 167.
[6] Seomum, S. S., Fukuda, T., Fukuda, A., Yoo, JHYPHENG., Panarin, YU. P., Vij, and , J. K., 2000, *J. mater. Chem.*, **10,** 2791.
[7] Chandani, A. D. L., Cui, Y., Seomun, S. S., Takanishi, Y., Ishikawa, K., Takezoe, H., and Fukuda, A., 1999, *Liq. Cryst.*, **26,** 168.
[8] Wu, S.-L., and Chiang, C. T., 2002, *Liq. Cryst.*, **29,** 39.
[9] Wu, S.-L., and Hsieh, W.-J., 2003, *Chem. Mater.*, **15,** 4515.
[10] Wu, S.-L., and Hsieh, W.-J., 1999, *Chem. Mater.*, **11,** 852.

[11] NISHIYAMA, I., and GOODBY, J. W., 1992, *J. mater. Chem.*, **2,** 1015.
[12] MIYASATO, K., ABE, S., TAKEZOE, H., FUKUDA, A., and KUZE, E., 1983, *Jpn. J. appl. Phys.*, **22,** L661.
[13] CHANDANI, A. D. L., HAGIWARA, T., SUZUKI, Y., OUCHI, Y., YAKAZOE, H., and FUKUDA, A., 1988, *Jpn. J. appl. Phys.*, **27,** L729.
[14] LEE, J., CHANDANI, A. D. L., ITOH, Y., TAKZOE, H., and FUKUDA, A., 1990, *Jpn. J. appl. Phys.*, **29,** 1122.
[15] WU, S. L., CHEN, D. G., HSIEH, W. J., YU, L. J., and LIANG, J. J., 1994, *Mol. Cryst. liq. Cryst.*, **250,** 153.
[16] KUCZYANSKI, W., and STEGEMEYER, H., 1994, *Ber. Bunnsenges. phys. Chem.*, **98,** 1322.
[17] KUCZYANSKI, W., and STEGEMEYER, H., 1995, *Mol. Cryst. liq. Cryst.*, **260,** 377.
[18] WU, S. L., and HSIEH, W. J., 1996, *Liq. Cryst.*, **21,** 783.
[19] BUIVYADS, M., GOUDA, F., ANDERSSON, G., LAGERWALL, S. T., STEBLER, B., BOMELBURG, J., HEPPKE, G., and GESTBLOM, B., 1997, *Liq. Cryst.*, **23,** 723.
[20] HIRAOKA, K., TAGUCHI, A., OUCHI, Y., TAKEZOE, H., and FUKUDA, A., 1990, *Jpn. J. appl. Phys.*, **29,** L103.
[21] GOUDA, F., SKARP, K., and LAGERWALL, S. T., 1991, *Ferroelectrics*, **113,** 165.
[22] GOODBY, J. W., BLINC, R., CLARK, N. A., LAGWEWALL, S. T., OSIPOV, M. A., PIKIN, S. A., SAKURAI, T., YOSHINO, K., and ZEKS, B., 1991, *Ferroelectric Liquid Crystals* (Gordon & Breach), p. 209.

Downloaded At: 16:42 25 January 2011